GEOPHYSICAL RESEARCH LETTERS, VOL. 25, NO. 9, PAGES 1317-1320, MAY 1, 1998

Detection of biomass burning combustion products in Southeast Asia from backscatter data taken by the GOME spectrometer

W. Thomas, E. Hegels and S. Slijkhuis

Deutsches Zentrum für Luft- und Raumfahrt (DLR), Oberpfaffenhofen, Germany

R. Spurr and K. Chance

Harvard-Smithsonian Center for Astrophysics, Cambridge, Massachusetts, USA

Abstract. We show that atmospheric UV/visible backscatter spectra obtained by the Global Ozone Monitoring Experiment (GOME) spectrometer on board the ESA ERS-2 satellite may be used to retrieve column amounts of key trace species associated with smoke cloud combustion from biomass burning events. This paper focuses on the recent rain forest burning in SE Asia (August-October 1997). For ground scenes with low cloudiness, differential absorption fitting applied to backscatter spectra yields column distributions of NO_2 and H_2CO in and around smoke-polluted regions. A two-fold increase in the vertical NO_2 content is apparent over large parts of the smoke cloud; this clearly indicates the ability of GOME to measure tropospheric NO_2 content. H_2CO is detected only in areas closest to combustion sources. Slant column amounts in the range 2.5 – 4×10^{16} mol cm^{-2} have been determined; these correspond with previous estimations of vertical columns of H_2CO for biomass Savannah burning.

Introduction

From early August to mid October 1997, a severe rain forest biomass burning event occurred in Southeast Asia. Wide areas of peninsular Malaysia, Borneo and Western Indonesia were frequently blanketed in dense clouds of smoke. Source fires were located in southern Borneo, in many locations on Java and eastern Sumatra, and in parts of Irian Jaya. Fires started as part of the traditional slash-and-burn agricultural cycle ran out of control, exacerbated by dry conditions and lack of monsoon rains (linked to the current El Niño event). Biomass burning events may be observed in a number of ways from space. Satellite sensors with high spatial resolution and a limited number of spectral channels can provide detailed visual information of the spatial distribution of smoke clouds. Highly-absorbing aerosols associated with biomass burning have been detected using the Total Ozone Mapping Spectrometer (TOMS) [*Hsu et al.*, 1996]. Spectrometers with moderate spectral resolution (such as GOME) can detect chemical tracer products of biomass combustion in the lower atmosphere.

The GOME spectrometer is an atmospheric chemistry instrument on board the European Space Agency's second European Remote Sensing satellite (ERS-2), launched in April 1995. In addition to its capability as an ozone instrument, GOME can also measure the atmospheric content of a number of minor but chemically important trace constituents including NO_2, H_2CO, BrO, OClO and SO_2. In this paper, we focus on the detection of biomass burning combustion products, with the main emphasis on the retrieval of column amounts of NO_2 and H_2CO from back-scatter spectra measured by GOME over SE Asia at the end of September 1997. In a biomass burning scenario, H_2CO concentrations are expected to be large in the troposphere, where hydrocarbon oxidation is greatly enhanced; in undisturbed atmospheres H_2CO is a product of the methane cycle. NO_2 is generated in natural (forest fires) and man-made (industrial production and heating, automobile combustion) burning processes. The distribution of NO_2 has a marked diurnal cycle and typically shows an enhanced tropospheric content. We show also that the ratio of GOME back-scatter radiances at 340 nm and 380 nm provides an indication of the presence of tropospheric smoke aerosol. Finally we report briefly on BrO and O_2-O_2 column amounts retrieved simultaneously with H_2CO and NO_2.

Data Processing and Retrieval

Back-scattered light from the earth's atmosphere entering the GOME spectrometer is registered by four 1024-pixel diode array detectors from 240 to 790 nm, with spectral resolutions of 0.2 to 0.4 nm. An extra-terrestrial solar spectrum is recorded (via a diffuser plate) at the same spectral resolution for a short time as the satellite emerges from the dark side of its sun-synchronous polar orbit (10h 30m mean local solar time at descending node). In normal operating mode, GOME is an across-track nadir-viewing sensor with a scan swath of $\pm$ 31°(corresponds to 960 km on ground). The full forward scan lasts 4.5 seconds, comprising three 1.5s steps with corresponding footprint sizes 320×40 km^2. The single fly-back scan lasts 1.5s. Global coverage is achieved in three days at the equator. For more details, see [*GOME Users Manual*, 1995].

The GOME Data Processor (GDP) performs the operational retrieval of trace constituents from nadir measurement spectra ([*Loyola et al.*, 1997]). The GDP was developed and designed at the German Remote Sensing Data Center (DLR-DFD) in collaboration with the Universities of Bremen and Heidelberg (Germany), and the Harvard-Smithsonian Center for Astrophysics (USA). Further contributions came from the Max Planck Institute of Chemistry (Mainz, Germany) and the Dutch Royal Meteorological Institute (KNMI, The Netherlands). The first part of GDP converts raw engineering data (level 0) to wavelength-calibrated, radiometrically corrected and geo-referenced backscatter radiances and solar spectrum irradiance values (level 1 data).

Paper number 98GL01087.
0094-8534/98/98GL-01087$05.00

The second part of GDP carries out the geophysical retrieval of atmospheric constituent amounts (level 2 data) by means of a number of component algorithms. The first of these determines the fractional cloud cover of the footprint from simulated atmospheric reflectances fitted to measurements in and around the O_2 *A* band (762 nm) ([*Kuze and Chance*, 1994]). The second algorithm is the core of level 1 to 2 processing; this is the DOAS (Differential Optical Absorption Spectroscopy) fitting technique for the retrieval of trace gas total column amounts along the instrument's viewing path ("slant columns") [*Platt et al.*, 1979]. A third component algorithm converts slant columns to geometry-independent vertical columns through division by appropriate air mass factors (AMFs). AMFs are derived from radiative transfer simulations based on atmospheric climatology and pixel geo-referencing information. For strongly absorbing species (e.g., O_3 in the Huggins bands) a full multiple scattering treatment is required. However, for NO_2, H_2CO and BrO in the present tropical scenario, the geometrical AMF approximation (sum of the solar zenith and line-of-sight secants) is sufficient.

The DOAS technique involves a multi-linear regression of GOME-measured optical densities against a number of background or reference spectra. For each trace gas, the reference spectrum is a set of laboratory-measured absorption cross-sections, and the fitting amplitude is then the effective slant column. The trace species path absorption is modeled on Beer's law; atmospheric attenuation due to Rayleigh scattering, particulate absorption and scattering and specular reflection are broad-scale features approximated by a low-order polynomial in wavelength. Fitting windows are optimized according to the principal trace species of interest. The DOAS fitting is improved when allowance is made for differences in wavelength registration between reference and measurement data; the multi-linear regression is then embedded in an iterative non-linear least-squares fitting process for the determination of wavelength shifts and squeezes (compressions) for the reference spectra.

For this biomass scenario, the NO_2 retrieval was performed in the operational processing environment, using a fitting window of 425-450 nm. Reference spectra include the NO_2 and O_3 absorption cross-sections, derived from measurements taken with the GOME flight model during the pre-launch calibration of the instrument. A "Ring" reference spectrum is also required, corresponding to spectral features produced by inelastic atmospheric scattering of solar Fraunhofer lines by N_2 and O_2 ([*Chance and Spurr*, 1997]); the Ring effect is treated as a pseudo-absorption in DOAS. The Ring spectrum was derived from pre-launch zenith-sky measurements with the GOME flight model, using the technique of [*Solomon et al.*, 1987]. All GOME flight model spectra were provided by the University of Bremen.

The retrieval of H_2CO was also carried out in the operational GDP environment, using the additional fitting window 336.5-357.5 nm ([*Perner et al.*, 1997]). There are six reference spectra (O_3 and NO_2 cross-sections and the Ring spectrum, plus cross-sections for BrO, H_2CO and the O_2-O_2 collision complex from other laboratory sources). For both the NO_2 and H_2CO applications, the GOME-measured solar spectrum was not fitted as a reference in the DOAS linear regression. However, the sun spectrum was included in the non-linear DOAS fitting; this ensures that the Ring reference spectra is properly wavelength-registered in the linear regression. The H_2CO fitting window coincides with part of the temperature-dependent Huggins O_3 absorption bands. Cross-sections for O_3 and NO_2 were obtained at a number of temperatures; 241K was selected for O_3, as being closest to atmospheric temperatures at that height where O_3 absorption reaches its maximum for wavelengths in the H_2CO fitting window. The same temperature was used for the NO_2 reference cross-sections. All back-scatter measurements were smoothed with a standard FFT filter, to remove high-frequency structures which may degrade the fitting.

Figure 1 shows detailed spectral output from one of the DOAS fits. The fitted differential absorption of H_2CO (reference cross-section multiplied by fitted slant path amplitude) is plotted against the residual H_2CO differential absorption (residual obtained from the measured spectrum after the subtraction of the broad-scale polynomial and all other differential absorbers except H_2CO). The two main absorption features of H_2CO are clearly present in the residual; remaining high frequency oscillations are due to instrument undersampling. The observed relative fitting error is reasonable, around 24%. This does not include additional errors in the H_2CO reference cross-section values (estimated to be at least 10%).

An indicator for the presence of tropospheric smoke aerosols is the ratio of averaged GOME backscatter measurements at 340 nm and 380 nm. These wavelengths are the same as those used for the TOMS absorbing aerosol index. Trace gas absorption is small between 340 nm and 380 nm, and for an unperturbed cloud-free atmosphere, the back-scatter spectrum is dominated by Rayleigh scattering, which decreases steadily with longer wavelengths (aerosol scattering and specular reflection signatures are normally flat between the two wavelengths). However, the soot-rich aerosols typical of large-scale biomass burning exhibit significant atmospheric absorption in this part of the spectrum (single scattering albedo typically 0.3); the absorption is higher for shorter wavelengths, and therefore low values of the 340-380 radiance ratio can indicate the presence of absorbing aerosols in the atmosphere. Even though the radiances at 340 and 380 nm have not been corrected for Rayleigh scattering, their ratios clearly correlate strongly with areas of enhanced NO_2 (see below).

For cloud-covered or partially cloudy scenes, indicators for the presence of smoke aerosols are compromised by the masking of the boundary layer. A maximum fractional cloud cover of 25% of the footprint was taken as the limit beyond which radiance ratios were not considered useful.

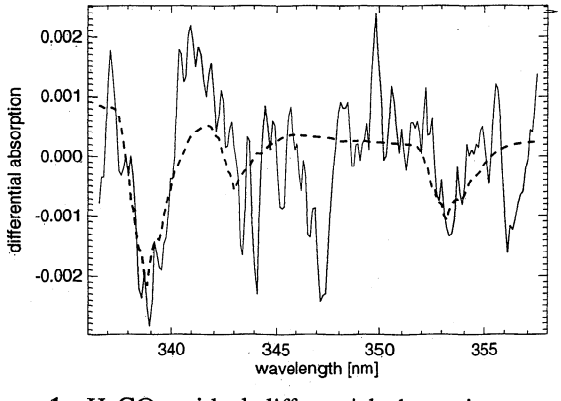

Figure 1. H_2CO residual differential absorption spectrum (solid line) and fitted absorption (dashed line) for a single nadir pixel over the burning area. [Solar zenith angle 20.5 degrees, direct nadir line-of-sight].

Since the biomass burning smog plume possesses greatly enhanced particulate loading, the large aerosol optical thickness in the lowest layers of the atmosphere may preclude the GOME instrument from seeing the ground. Retrieved trace gas columns may not reflect the total atmospheric content. Enhanced aerosol loading in the boundary layer will also affect the AMF calculation. Column amounts are therefore likely to be underestimates of their true values.

Biomass Burning Results

A series of GOME overpasses for the period 26-28 September were analyzed for NO_2 and H_2CO content. Figure 2 (top panel) shows the fractional cloud cover for a single orbit over Java and Borneo on September 27. In the region of interest, the cloudiness is generally low (below 30%); the troposphere is not obscured by optically thick clouds. The low cloud content was confirmed by an examination of contemporaneous NOAA-14 AVHRR visible images provided by the Meteorological Service of Singapore.

Figures 3 and 4 show vertical columns of NO_2 and slant column amounts of H_2CO respectively, for two different orbits over Java and Borneo on September 27. All three forward scans were used for NO_2 retrievals, whereas only the central (nadir) forward scan measurements were fitted for H_2CO. Areas of enhanced NO_2 and H_2CO are shown in red. The southern coastline of Borneo clearly demarcates the region of enhanced NO_2. A similar enhanced NO_2 effect is also observed for Java. The H_2CO distribution is similar, but the enhancement less pronounced; only in areas where the presence of H_2CO is strongly enhanced is it possible to distinguish its absorption signature. Outside areas close to combustion sources, the H_2CO slant column retrieval uncertainties are too high for the results to be useful. A more detailed view of the data is presented in Figure 2, where in addition to the fractional cloud cover, the 340-380 radiance ratios and the distributions of NO_2 (vertical column) and H_2CO (slant column) are shown as functions of latitude for a part of one orbit. There is a deep and clear minimum in the radiance ratio values over the smoke-covered region, and this coincides with regions of enhanced H_2CO and NO_2 content. Subtraction of the Rayleigh component from the radiances

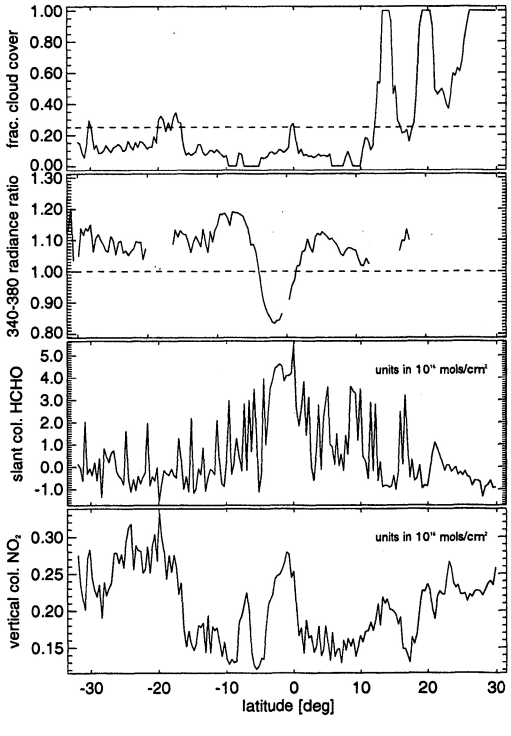

Figure 2. Fractional cloud cover (top panel), 340-380 nm radiance ratio (second panel), slant column of H_2CO (third panel) and vertical column of NO_2 (fourth panel) over Indonesia for 27 September 1997, as a function of latitude.

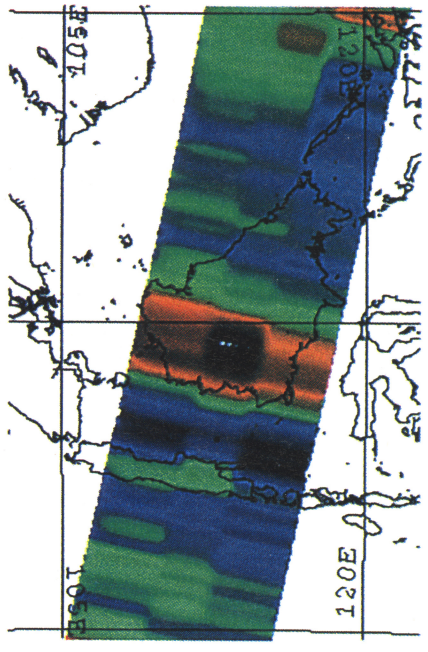

Figure 3. Vertical column of NO_2 over Indonesia for 27 September 1997. Maximum concentrations around 2.5×10^{15} mol cm^{-2} are colored in red.

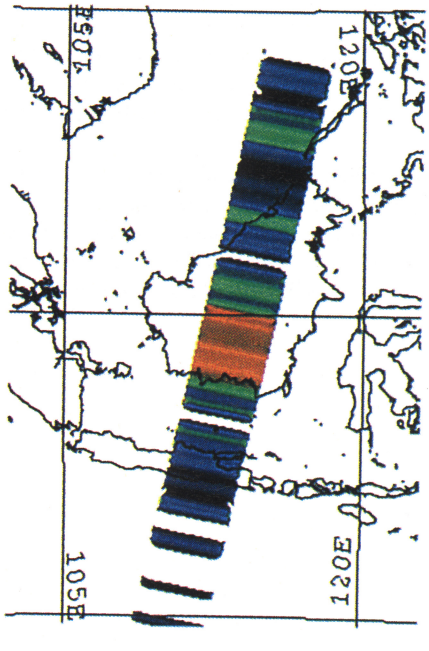

Figure 4. Slant column of H_2CO over Indonesia for 27 September 1997. Maximum concentrations around 4×10^{16} mol cm^{-2} are colored in red.

would displace the ratios downwards slightly (closer to unity for those pixels outside the smoke regions), but would not mask the large indication of absorbing aerosols.

There are two relative maxima in the NO_2 concentration over Java (latitude around -8°S) and Southern Borneo (between -5°S and +1°N). In the tropical atmosphere, the NO_2 vertical column content is usually low (typically around 1.2×10^{15} mol cm^{-2}). Over Southern Borneo the NO_2 concentration increases by more than a factor of 2, giving a total content around $2.5\times10^{15} \pm 0.8\times10^{15}$ mol cm^{-2}, with the enhancement attributable to biomass burning. The first relative maximum at -7°S corresponds to Java. For an unperturbed tropical atmosphere, most of the total NO_2 vertical column content is in the stratosphere. Here, the enhanced tropospheric content of NO_2 above the lowest observable atmospheric layer is of the same order as the complete stratospheric content. Since GOME may not be observing the planetary boundary layer because of the smog, this tropospheric NO_2 content may well be an underestimate.

The slant column content of H_2CO over Southern Borneo lies in the range $2.5 - 4 \times 10^{16} \pm 0.9 \times 10^{16}$ mol cm^{-2}. The retrieved column amount of H_2CO over Java is not as high; this is probably due to the reduced biomass (limited rain forest, predominantly agricultural landscapes). With the geometric air mass factor correction to account for the slant path enhancement of absorption, we estimate the corresponding vertical column for H_2CO to be around $1.5 - 2\times10^{16}$ mol cm^{-2}. These compare with results for the vertical H_2CO content presented by [*Perner et al.*, 1997] for burning African Savannah; our results are higher, reflecting the higher biomass content of the Borneo tropical rain forest.

Since BrO and O_2-O_2 have absorption bands in the H_2CO fitting window, their slant columns were determined simultaneously for these GOME overpass orbits. The slant column content of BrO was $6.5\times10^{13} \pm 2.5\times10^{13}$ mol cm^{-2} at a sun zenith angle of 21°. Although this fitting window is not optimal for BrO retrieval, these results are comparable to values given by [*Hegels et al.*, 1996]. For the measured content of BrO, no correlation with the haze clouds could be found. The observed spatial distribution of O_2-O_2 correlates reasonably well with the cloud cover; this is to be expected, since the pressure-squared dependency of the O_2-O_2 collision complex atmospheric concentration restricts significant absorption of this species to the lower troposphere.

Acknowledgments. Special thanks to T. Kluepfel (Max-Planck Institute for Chemistry, Mainz, Germany) for contributions regarding H_2CO fitting. A. Ladstaetter-Weißenmayer, D. Perner, U. Platt and M. Eisinger also contributed to development of trace gas retrieval from GOME data. Thanks also to J. Burrows (University of Bremen), the lead scientist on GOME. We are grateful to C. Bilinski, T. Ruppert and other members of the GOME Team at DLR-DFD for help with data processing. The Meteorological Office at Singapore are kindly acknowledged for providing the NOAA-14 AVHRR data and additional information on wind fields and smoke cloud thickness. We are grateful to anonymous reviewers whose comments helped to improve the paper.

References

Chance K. and R. J. D. Spurr, Ring Effect Studies: Rayleigh Scattering, including Molecular Parameters for Rotational Raman Scattering, and the Fraunhofer Spectrum, *Applied Optics* 36, 5224-5230, 1997

GOME (Global Ozone Monitoring Experiment) Users Manual, European Space Agency, SP-1182, 1995

Kuze A. and K. V. Chance, Analysis of Cloud-Top Height and Cloud Coverage from Satellites Using the O_2 A and B Bands, *J. Geophys. Res.* 99, 14481-14491, 1994

Hsu N., J. Herman, P. Bhartia, C. Seftor, O. Torres, A. Thompson, J. Gleason, T. Eck and B. Holben, Detection of Biomass Burning Smoke from TOMS measurements, *Geophys. Res. Lett.* 23, 745-748, 1994

Hegels, E., P. J. Crutzen, T. Kluepfel, D. Perner, J. P. Burrows, A. Ladstaetter-Weissenmayer, M. Eisinger, J. Callies, A. Hahne, K. Chance, U. Platt and W. Balzer, Satellite measurements of halogen oxides by the Global Ozone Monitoring Experiment, GOME, on ERS2: Distribution of OClO and BrO and comparison with groundbased observations, *XVIII Quadrennial Ozone Symposium*, Vol. Abstracts, p 229, L'Aquila, Italy, 12-21 September, 1996

Loyola D., B. Aberle, W. Balzer, K. Kretschel, E. Mikusch, H. Muehle, T. Ruppert, C. Schmid, S. Slijkhuis, R. Spurr, W. Thomas, T. Wieland and M. Wolfmueller, Ground Segment for ERS-2 GOME Data Processor, *Proceedings of the 3rd ERS-2 Users Conference*, Florence, Italy, 1997 (in press)

Platt U., D. Perner and H. W. Paetz, Simultaneous Measurement of atmospheric CH_2O, O_3, and NO_2 by differential optical absorption, *J. Geophys. Res*, 84, 6329-6335, 1979.

Perner D., T. Kluepfel, E. Hegels, P. J. Crutzen and J. P. Burrows, First Results on Tropospheric Observations by the Global Ozone Monitoring Experiment, GOME, on ERS 2, *Proceedings of the 3rd ERS-2 Users Conference*, Florence, Italy, 1997

Solomon S., A. L. Schmeltekopf and R. W. Sanders, On the interpretation of zenith sky absorption measurements, *J. Geophys. Res*, 92, 8311-8319, 1987.

W. Thomas, E. Hegels and S. Slijkhuis, Deutsches Fernerkundungsdatenzentrum (DLR-DFD), Oberpfaffenhofen, Germany. (e-mail: Werner.Thomas@dlr.de)

R. Spurr and K. Chance, Harvard–Smithsonian Center for Astrophysics, Cambridge, Massachusetts, USA. (e-mail: rspurr@cfa.harvard.edu)

(Received November 27, 1997; revised February 16, 1998; accepted March 27, 1998.)